JOURNAL OF SOLID STATE CHEMISTRY 46, 46–55 (1983)

X-Ray Study of a Mixed Indium Chalcogenide $In_{\sim 2.01}X_3$ (X = S, Se, Te): The Occurrence of Indium(I) in Indium(III) Chalcogenides

C. SVENSSON AND J. ALBERTSSON

Inorganic Chemistry 2, Chemical Center, University of Lund, P.O.B. 740, S-220 07, Lund, Sweden

Received April 5, 1982

The mixed indium chalcogenide semiconductor $In_{\sim 2.01}X_3$ (X = S, Se, Te) crystallizes in trigonal space group $R\bar{3}$ with a = 14.003(1), c = 35.228(5) Å and V = 5982(1) Å^3 at room temperature. X-Ray intensities were collected with a four-circle single-crystal diffractometer and the structure was solved by direct methods. The least-squares refinement converged to R = 0.061. The unit cell content was found to be $In^{I}In^{III}(oct)_3In^{III}(tetr)_{73}X_{115}$ with an apparent chalcogen ratio Se : Te = 2.22 : 3 (S : Se : Te ≈ 1 : 2 : 3 from electron microprobe analysis). The chalcogen octahedron around one type of In^{III} atom shares edges with six distorted In^{III}–X tetrahedra. These units are connected in three dimensions by other edge- and corner-sharing In^{III}–X tetrahedra. One octahedral cavity is formed by disordered chalcogen atoms. One-third of these cavities are unoccupied, another one-third are occupied by In^{I} in one-sided coordination, and the last one-third are occupied by In^{III} and a chalcogen atom so that In^{III} is in a tetrahedral environment. The possible exchange of some In^{III} for In^{I} in various indium chalcogenide compounds is discussed.

Introduction

In a search for new semiconducting materials Titze (*1*) recently made a series of syntheses with elemental indium and chalcogen mixtures as starting material. Among the various phases obtained one had the approximate composition $In_4SSe_2Te_3$ (corresponding to In_2X_3). To our knowledge this is the first indium chalcogenide containing all three of S, Se, and Te. In order to clarify its structure an X-ray diffraction analysis was undertaken.

The crystal chemistry of the indium chalcogenides is complicated (*2, 3*) but most of the In_2X_3 compounds are based on comparatively simple structure types. Thus, among the low-temperature phases, β-In_2S_3 is a defect spinel (*4*), γ-In_2Se_3 is related to wurtzite (*5*), and γ-In_2Te_3 adopts a random zinkblende structure (*6*). As shown below, the present compound includes a small amount of In^{I} and may be formulated $In_{\sim 2.01}X_3$. Its structure is fairly complicated. A literature survey based on the characteristics of In^{I} in our structural model indicates that other indium chalcogenides probably also contain small amounts of In^{I}. Some implications of this In^{I} coordination on the crystal chemistry of indium are discussed.

Experimental

The black title compound was synthesized in an evacuated quartz tube by heating a mixture of the pure elements with molar ratios In : S : Te ≈ 2 : 1 : 1 : 1 (*1*). Single crystals were grown by sublimation of the

0022-4596/83/010046-10$03.00/0

reaction product using a small temperature gradient in the preparation tube. An electron microprobe analysis gave the approximate composition $In_4SSe_2Te_3$. A stout prismatic crystal with dimensions of 0.10 × 0.15 × 0.08 mm was used for the crystallographic investigation.

The solution of the structure and the preliminary refinement was based upon a triclinic unit cell (space group $P\bar{1}$), but then it became evident that the structural model should include a threefold axis. The true space group should be $R\bar{3}$. Unit cell data are given in Table I and the relations between the various cells referred to in this paper are given in Fig. 1. The cell dimensions are determined by least-squares from the θ angles of 47 reflections measured on a CAD4 diffractometer with Zr-filtered Mo$K\alpha_1$ radiation ($\lambda K\alpha_1$ = 0.70930 Å).

The intensity data in a hemisphere of reciprocal space with radius sin θ/λ = 0.64 $Å^{-1}$ were measured with ω scans. The angular range was 0.8° + 0.5° tan θ. The maximum scan time of 120 sec resulted in $\sigma_c(I)/I \leq 0.03$ ($\sigma_c(I)$ is based on counting statistics). The intensities of two standard reflections were measured every 2 hr; no systematic variations were detected. A total of 9038 structure factors were measured, of which 4337 had $I > 3\sigma_c(I)$ and were regarded as observed. Corrections were made for Lorentz, polarization, and absorption effects; the transmission factors were in the range 0.16–0.29.

TABLE I

UNIT CELL DIMENSIONS (SEE FIG. 1)

Space group $R\bar{3}$
Hexagonal axes:
a_H = 14.003(1), c_H = 35.228(5) Å, V_H = 5982(1) $Å^3$
Rhombohedral axes:
a_R = 14.257(2) Å, α_R = 58.85(1)°, V_R = 1994(1) $Å^3$
Pseudocell, space group $R\bar{3}$
Hexagonal axes:
$a'_H = a_H$, $c'_H = c_H/2$
Rhombohedral axes:
a'_R = 9.992 Å, α'_R = 88.97°
Triclinic cell, space group $P\bar{1}$
$\mathbf{a}_T = \mathbf{a}_H$, $\mathbf{b}_T = -\mathbf{b}_H$, $\mathbf{c}_T = -\mathbf{b}_R$

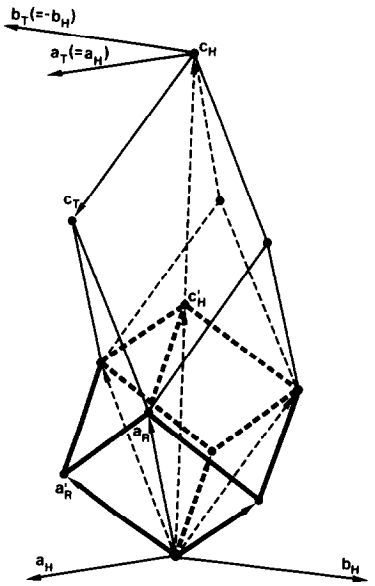

FIG. 1. Relationships between the unit cells used to describe the structure (cf. Table I); H: hexagonal; R: rhombohedral; and T: triclinic axes.

Solution and Refinement of the Structure

The structure was solved in space group $P\bar{1}$ by direct methods (*7*). The intensity statistics indicated a hypercentric distribution. The E-map based on the phase set with highest combined figure of merit revealed the structure. Its 40 most prominent peaks were assumed to be atomic sites and these were least-squares refined using the Se scattering factor for all the atoms. The resulting isotropic thermal parameters and interatomic distances were used to assign the atoms as In, Se, or Te. Further least-squares cycles and difference electron density calculations gave a reasonable model of the structure containing 33 independent atoms. All attempts to include S atoms in the model resulted in negative temperature factor coefficients, indicating a higher actual electron density than assumed. In the fol-

TABLE II

STRUCTURAL REFINEMENT INDICATORS (NO. OF REFLEXIONS: $n = 4337$, $\Delta F = |F_o| - |F_c|$)

Refinement (see text)	*A*	*B*	*C*
No. of parameters, m	287	101	115
$R = \Sigma\|\Delta F\|/\Sigma\|F_o\|$	0.071	0.066	0.0606
$R_w = [\Sigma w(\Delta F)^2/\Sigma w\|F_o\|^2]^{1/2}$	0.105	0.091	0.0845
$S = [\Sigma w(\Delta F)^2/(n-m)]^{1/2}$	2.67	1.13	1.047
C_1 (weighting function)	0.03	0.05	0.05
C_2 (weighting function)	—	600	600
$g \times 10^{-2}$	—	3.5(5)	3.5(4)

lowing the chalcogen atoms are designated by *X* followed by the element symbol for the scattering factors used in the refinements.

The function minimized in the least-squares refinement was $\Sigma w(|F_o| - |F_c|)^2$ with weights calculated from $w^{-1} = \sigma_c^2(|F_o|) + (C_1|F_o|)^2 + C_2$. All atoms in the model were allowed to vibrate anisotropically within the harmonic approximation. Atomic scattering factors and anomalous dispersion corrections for the neutral atoms were taken from *International Tables for X-Ray Crystallography* (*8*). Table II gives the structural refinement indicators.

When the first series of least-squares cycles (*A*) had converged the threefold axis was detected and space group $R\bar{3}$ verified (*B*). In both the applied models the In(1) atom and its nearest neighbors are disordered. The thermal ellipsoids of the chalcogen *X*Te(5) was extended perpendicular to the threefold axis, with the same appearance at the three independent sites in the $P\bar{1}$ model. The electron density could be resolved into two atomic sites in the final refinement (*C*) and a further Se atom was introduced on the threefold axis at the location of the major residual electron density. In refinements *B* and *C* the data set was tested for isotropic extinction (*9*). The maximum correction applied on $|F_o|$ was 1.28 for reflexion $1\,\bar{3}\,\bar{8}$. The highest residual in the final difference electron density map was 1.9 e Å^{-3} near In(4) but there is also a trough about 3 e Å^{-3} deep near *X*Se(1).

Final atomic parameters are given in Tables III and IV. A list of observed and cal-

TABLE III

ATOMIC POSITIONAL COORDINATES IN THE HEXAGONAL UNIT CELL OF $In_{\sim 2.01}X_3$

Atom	*x*	*y*	*z*	*B* (Å^2)	Occupancy
In(1)	0	0	0.98356(26)	3.04(23)	0.34(1)
In(2)	0	0	½	1.77(7)	
In(3)	0.5134(1)	0.5520(1)	0.95205(4)	1.73(4)	
In(4)	0.4435(1)	0.5908(1)	0.44986(4)	1.70(4)	
In(5)	0.4637(1)	0.0166(1)	0.84021(4)	1.72(4)	
In(6)	0.4680(1)	0.0139(1)	0.34713(4)	2.11(5)	
*X*Se(1)	0	0	0.25279(14)	4.08(11)	
*X*Se(2)	0.4084(2)	0.4317(2)	0.89513(8)	3.71(9)	
*X*Se(3)	0.4147(2)	0.4268(2)	0.40519(7)	2.95(7)	
XSe(4)	0	0	0.05919(87)	7.5(1.8)	0.18(2)
*X*Te(5A)	0.2309(8)	0.1651(6)	0.95326(10)	4.18(27)	0.67(2)
*X*Se(5B)	0.2899(11)	0.2124(11)	0.95367(27)	1.76(28)	0.33
*X*Te(6)	0.1957(1)	0.1461(1)	0.45289(4)	2.57(5)	
*X*Te(7)	0.6306(1)	0.4713(1)	0.99040(4)	2.40(4)	
*X*Te(8)	0.6390(1)	0.4852(1)	0.48032(4)	2.14(4)	

Note. The elemental symbol after *X* denotes the type of form factor used for the chalcogen. The *B* values were calculated from the anisotropic temperature factor coefficients.

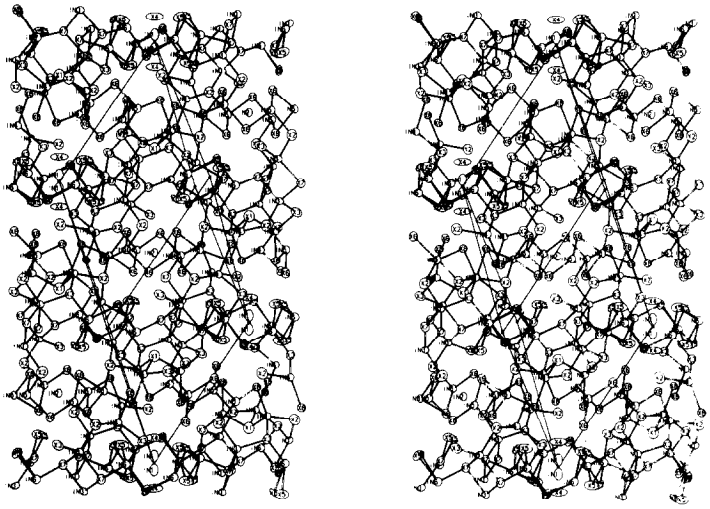

FIG. 2. A stereoview of the structure of $In_{\sim 2.01}X_3$. Hexagonal [110] points toward the reader. Rhombohedral cell is shown. The thermal ellipsoids are scaled to include 75% probability.

culated structure factors is available.[1] The chalcogen thermal parameters are somewhat large, and their average isotropic rms value is 0.180 Å. This and the approximate composition $In_4SSe_2Te_3$ found in the microprobe analysis indicate that the atoms assigned here as *X*Se are actually a distribution of S and Se atoms while the *X*Te atoms are a distribution of Se and Te. The trough near *X*Se(1) is probably caused by a disorder of this atom and/or the distribution of S and Se on this site. Part of the thermal smearing is then probably a result of the model which gives an electron density that is too high at the chalcogen sites.

[1] See NAPS document No. 03999 for 17 pages of supplementary material. Order from ASIS/NAPS, c/o Microfiche Publications, P.O. Box 3513, Grand Central Station, New York, New York 10017. Remit in advance for each NAPS Accession number. Institutions and organizations may use purchase orders when ordering, however, there is a billing charge for this service. Make checks payable to Microfiche Publications. Photocopies are $7.75. Microfiche are $4.00. Outside of U.S. and Canada, postage is $4.50 for a photocopy or $1.50 for a fiche.

Description of the Structure

A stereoscopic pair of drawings of the crystal structure is shown in Fig. 2. Table V gives selected interatomic distances and Table VI bond angles. The disorder of In(1) and its neighborhood will be described below. In(2) is octahedrally coordinated by the *X*Te(6) atoms and In(3)–In(6) are in tetrahedral interstices formed by *X*Se and *X*Te. Each chalcogen atom except *X*Se(4), *X*Se(5B), and *X*Te(8) has three bonds to In atoms. *X*Se(4) and *X*Se(5B) are associated with the In(1) disorder and have one and two In neighbors, respectively. *X*Te(8) is bonded to two In atoms.

The averaged tetrahedral In–*X*Se bond distance is 2.62(4) Å and the corresponding In–*X*Te distance is 2.75(4) Å, excluding distances to disordered atoms. The octahedral In(2)–*X*Te(6) bond distance is 2.974(1) Å, i.e., the distance is 0.22(4) Å larger for coordination number six than for coordination number four, as could be expected from the In^{3+} ionic radii (*10*). The small difference between the tetrahedral In–*X*Se and In–*X*Te bond lengths, 0.13(6) Å, might reflect

TABLE IV

ANISOTROPIC THERMAL PARAMETERS OF $In_{\sim 2.01}X_3$

Atom	U_{11}	U_{22}	U_{33}	U_{12}	U_{13}	U_{23}
In(1)	0.0282(34)	U_{11}	0.0590(55)	$U_{11}/2$	0	0
In(2)	0.0185(10)	U_{11}	0.0299(18)	$U_{11}/2$	0	0
In(3)	0.0235(7)	0.0203(7)	0.0189(7)	0.0087(6)	−0.0024(5)	0.0021(5)
In(4)	0.0195(7)	0.0191(7)	0.0201(7)	0.0051(6)	0.0020(5)	0.0014(5)
In(5)	0.0216(7)	0.0158(6)	0.0270(7)	0.0088(6)	0.0020(5)	0.0024(5)
In(6)	0.0249(8)	0.0295(8)	0.0269(8)	0.0143(6)	0.0004(6)	0.0021(6)
*X*Se(1)	0.0498(16)	U_{11}	0.0553(29)	$U_{11}/2$	0	0
*X*Se(2)	0.0413(14)	0.0500(15)	0.0497(15)	0.0229(13)	−0.0008(12)	−0.0055(12)
*X*Se(3)	0.0269(12)	0.0393(13)	0.0361(12)	0.0092(10)	0.0030(9)	−0.0085(10)
*X*Se(4)	0.132(31)	U_{11}	0.019(17)	$U_{11}/2$	0	0
*X*Te(5A)	0.0965(58)	0.0675(39)	0.0325(15)	0.0693(44)	−0.0113(20)	−0.0049(16)
*X*Se(5B)	0.0225(50)	0.0281(47)	0.0256(35)	0.0195(43)	0.0132(31)	0.0180(31)
*X*Te(6)	0.0313(8)	0.0312(8)	0.0371(8)	0.0172(7)	0.0004(6)	0.0034(6)
*X*Te(7)	0.0270(7)	0.0290(7)	0.0347(8)	0.0136(6)	−0.0009(6)	0.0049(6)
*X*Te(8)	0.0266(7)	0.0252(7)	0.0239(7)	0.0087(6)	0.0003(5)	0.0030(5)

Note. The form of the anisotropic temperature factor is $\exp[-2\pi^2(U_{11}h^2a^{*2} + \ldots)]$. See also the heading of Table I.

the presumed distribution of Se and Te atoms on the *X*Te sites and of S and Se on the *X*Se sites. Tables V and VI show that the octahedron about In(2) is slightly flattened along $\mathbf{c}_H$ and that the tetrahedra about In(3)–In(6) are very distorted: In(5) represents the extreme case with bond angles in the interval 91–137° and with the tetrahedral edges ranging from 3.85 to 5.06 Å. The average In–*X*Se–In bond angle is 101(3)°, a value that decreases to 89(5)° for In–*X*Te–In. The shortest In–In distance is 3.623(3) Å between two In(3) atoms in edge-sharing coordination polyhedra. It is noteworthy that the *X*–*X* distances are in general shorter when the chalcogen atoms are not bonded to the same In atom (Table V).

The heavy distortion of the InX_4 tetrahedra is caused by the span in chalcogen sizes and leads to a rather complicated connectivity in the compound (Fig. 2). Apparently, there is no simple way to delineate the structure. The approach used here is based on the pseudosymmetry revealed by the approximate equivalence between positions

TABLE V

SELECTED INTERATOMIC DISTANCES (Å) (ATOMS 5A AND 5B ARE NOT PRESENT SIMULTANEOUSLY)

In(1) polyhedron			In(3) polyhedron continued		
In(1)–*X*Se(4)		2.664(32)	*X*Te(7)–*X*Te(7)		4.175(3)
In(1)–*X*Te(5A)	3×	3.076(9)	In(3)–In(3)		3.623(3)
In(1)–*X*Te(5A)	3×	3.644(9)	In(3)–In(4)		3.936(2)
*X*Se(4)–*X*Te(5A)	3×	4.717(10)	In(3)–In(5)		4.000(2)
*X*Te(5A)–*X*Te(5A)	3×	4.998(8)	In(3)–In(6)		4.147(2)
In(1)–In(6)	3×	3.912(2)			
In(1)–In(6)	3×	4.054(3)	In(4) polyhedron		
			In(4)–*X*Se(1)		2.599(3)
			In(4)–*X*Se(2)		2.560(3)
In(2) polyhedron			In(4)–*X*Se(3)		2.643(3)
			In(4)–*X*Te(8)		2.699(2)
In(2)–*X*Te(6)	6×	2.974(1)	*X*Se(1)–*X*Se(2)		4.016(3)
*X*Te(6)–*X*Te(6)	6×	4.136(3)	*X*Se(1)–*X*Se(3)		4.063(2)
*X*Te(6)–*X*Te(6)	6×	4.273(3)	*X*Se(1)–*X*Te(8)		4.403(4)
In(2)–In(5)	6×	3.899(1)	*X*Se(2)–*X*Se(3)		4.115(4)
			*X*Se(2)–*X*Te(8)		4.627(3)
			*X*Se(3)–*X*Te(8)		4.391(3)
			In(4)–In(4)	2×	3.931(2)
In(3) polyhedron			In(4)–In(5)		3.933(2)
			In(4)–In(6)		4.125(2)
In(3)–*X*Se(2)		2.558(3)			
In(3)–*X*Se(3)		2.594(3)	In(5) polyhedron		
In(3)–*X*Te(7)		2.762(2)			
In(3)–*X*Te(7)		2.766(2)	In(5)–*X*Se(2)		2.649(3)
*X*Se(2)–*X*Se(3)		4.194(4)	In(5)–*X*Te(6)		2.732(2)
*X*Se(2)–*X*Te(7)		4.376(3)	In(5)–*X*Te(6)		2.736(2)
*X*Se(2)–*X*Te(7)		4.419(3)	In(5)–*X*Te(8)		2.707(2)
*X*Se(3)–*X*Te(7)		4.621(3)	*X*Se(2)–*X*Te(6)		4.328(3)
*X*Se(3)–*X*Te(7)		4.317(3)	*X*Se(2)–*X*Te(6)		3.851(3)

TABLE V—*Continued*

In(5) polyhedron continued		
*X*Se(2)–*X*Te(8)		4.304(3)
*X*Te(6)–*X*Te(6)		4.136(3)
*X*Te(6)–*X*Te(8)		4.521(3)
*X*Te(6)–*X*Te(8)		5.059(3)
In(5)–In(5)	2×	3.922(1)
In(6) polyhedron		
In(6)–*X*Se(3)		2.650(3)
In(6)–*X*Te(5A)		2.683(7)
In(6)–*X*Te(5A)		2.690(6)
In(6)–*X*Se(5B)		2.614(11)
In(6)–*X*Se(5B)		2.667(13)
In(6)–*X*Te(7)		2.825(2)
*X*Se(3)–*X*Te(5A)		3.966(9)
*X*Se(3)–*X*Te(5A)		4.422(5)
*X*Se(3)–*X*Te(7)		4.454(3)
*X*Te(5A)–*X*Te(5A)		4.378(8)
*X*Te(5A)–*X*Te(7)		4.409(9)
*X*Te(5A)–*X*Te(7)		4.874(9)
*X*Se(3)–*X*Se(5B)		4.221(10)
*X*Se(3)–*X*Se(5B)		4.120(14)
*X*Se(5B)–*X*Se(5B)		4.890(17)
*X*Se(5B)–*X*Te(7)		3.986(13)
*X*Se(5B)–*X*Te(7)		4.451(13)
In(6)–In(6)	2×	4.030(2)
Other *X*–*X* contact distances less than 4.0 Å		
*X*Se(1)–*X*Te(7)	3×	3.879(4)
*X*Se(2)–*X*Se(5B)		3.368(12)
*X*Se(2)–*X*Te(8)		3.858(3)
*X*Se(2)–*X*Te(5A)		3.877(7)
*X*Se(2)–*X*Te(6)		3.970(3)
*X*Se(3)–*X*Te(8)		3.869(3)
*X*Se(3)–*X*Te(5A)		3.878(8)
*X*Se(3)–*X*Te(6)		3.952(3)
*X*Se(3)–*X*Te(5A)		3.966(9)
*X*Se(4)–*X*Se(5B)	3×	3.668(14)
*X*Se(4)–*X*Te(8)	3×	3.881(24)
*X*Te(5A)–*X*Te(8)		3.737(5)
*X*Se(5B)–*X*Te(6)		3.755(12)
*X*Se(5B)–*X*Te(8)		3.954(11)
*X*Se(5B)–*X*Te(7)		3.986(14)
*X*Te(7)–*X*Te(7)	2×	3.858(2)

TABLE VI

BOND ANGLES (°) (SEE ALSO THE HEADING OF TABLE V)

*X*Se(4)–In(1)–*X*Te(5A)	3×	108.6(2)
*X*Te(5A)–In(1)–*X*Te(5A)	3×	110.3(2)
*X*Te(6)–In(2)–*X*Te(6)	6×	91.9(1)
*X*Te(6)–In(2)–*X*Te(6)	6×	88.1(1)

TABLE VI—*Continued*

*X*Se(2)–In(3)–*X*Se(3)		109.0(1)
*X*Se(2)–In(3)–*X*Te(7)		110.6(1)
*X*Se(2)–In(3)–*X*Te(7)		112.1(1)
*X*Se(3)–In(3)–*X*Te(7)		119.3(1)
*X*Se(3)–In(3)–*X*Te(7)		107.3(1)
*X*Te(7)–In(3)–*X*Te(7)		98.1(1)
*X*Se(1)–In(4)–*X*Se(2)		102.2(1)
*X*Se(1)–In(4)–*X*Se(3)		101.6(1)
*X*Se(1)–In(4)–*X*Te(8)		112.4(1)
*X*Se(2)–In(4)–*X*Se(3)		104.5(1)
*X*Se(2)–In(4)–*X*Te(8)		123.2(1)
*X*Se(3)–In(4)–*X*Te(8)		110.5(1)
*X*Se(2)–In(5)–*X*Te(6)		107.1(1)
*X*Se(2)–In(5)–*X*Te(6)		91.3(1)
*X*Se(2)–In(5)–*X*Se(8)		107.0(1)
*X*Te(6)–In(5)–*X*Te(6)		98.3(1)
*X*Te(6)–In(5)–*X*Te(8)		112.4(1)
*X*Te(6)–In(5)–*X*Te(8)		136.7(1)
*X*Se(3)–In(6)–*X*Te(5A)		96.1(2)
*X*Se(3)–In(6)–*X*Te(5A)		111.8(2)
*X*Se(3)–In(6)–*X*Te(7)		108.8(1)
*X*Te(5A)–In(6)–*X*Te(5A)		109.2(3)
*X*Te(5A)–In(6)–*X*Te(7)		124.5(2)
*X*Te(5A)–In(6)–*X*Te(7)		106.1(2)
*X*Se(3)–In(6)–*X*Se(5B)		106.6(3)
*X*Se(3)–In(6)–*X*Se(5B)		101.6(2)
*X*Se(5B)–In(6)–*X*Se(5B)		135.7(5)
*X*Se(5B)–In(6)–*X*Te(7)		94.2(3)
*X*Se(5B)–In(6)–*X*Te(7)		108.3(3)
In(4)–*X*Se(1)–In(4)	3×	98.2(1)
In(3)–*X*Se(2)–In(4)		103.3(1)
In(3)–*X*Se(2)–In(5)		100.4(1)
In(4)–*X*Se(2)–In(5)		103.8(1)
In(3)–*X*Se(3)–In(4)		97.5(1)
In(3)–*X*Se(3)–In(6)		104.5(1)
In(4)–*X*Se(3)–In(6)		102.4(1)
In(1)–*X*Te(5A)–In(6)		85.3(2)
In(1)–*X*Te(5A)–In(6)		89.1(2)
In(6)–*X*Te(5A)–In(6)		97.2(1)
In(6)–*X*Se(5B)–In(6)		99.5(3)
In(2)–*X*Te(6)–In(5)		86.1(1)
In(2)–*X*Te(6)–In(5)		86.0(1)
In(5)–*X*Te(6)–In(5)		91.7(1)
In(3)–*X*Te(7)–In(3)		81.9(1)
In(3)–*X*Te(7)–In(6)		95.6(1)
In(3)–*X*Te(7)–In(6)		94.9(1)
In(4)–*X*Te(8)–In(5)		93.4(1)

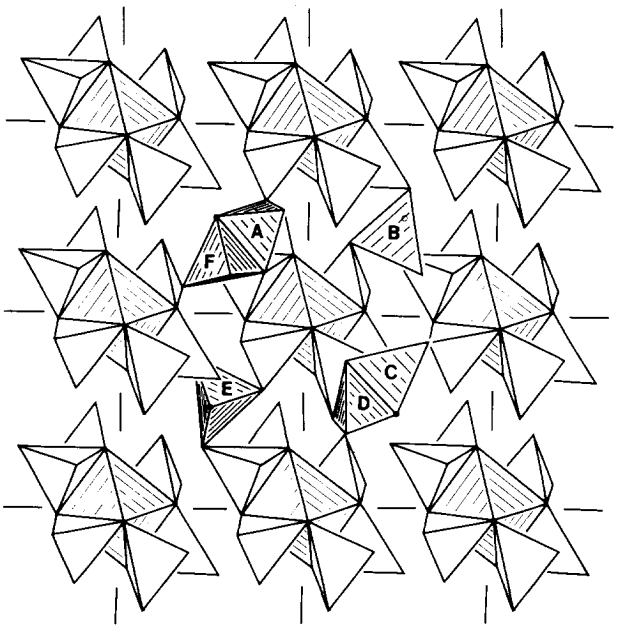

FIG. 3. The averaged structure, viewed along rhombohedral a'_R. The tetrahedra A–F form one complete environment of the Se atom at $\frac{1}{2}\ \frac{1}{2}\ \frac{1}{2}$ (●); B and C are pointing downwards. In the real structure either of the sets A,B,C or D,E,F is occupied by In (cf. the text). The threefold axis along the body diagonal goes from the lower left to the upper right in the drawing.

x, y, z and $x, y, z + \frac{1}{2}$ in the list of atomic coordinates (Table III). The pseudosymmetry elements are $\bar{3}$ at 0, 0, $\frac{1}{4}$ and $\bar{1}$ at $\frac{1}{2}$, 0, $\frac{1}{4}$ and $\frac{1}{6}$, $\frac{1}{3}$, $\frac{1}{6}$. An "averaged" structure with space group $R\bar{3}$ can be located in a hexagonal unit cell a_H, b_H, $c'_H = c_H/2$ or the corresponding rhombohedral cell in the reverse setting with $a'_R = 9.99$ Å and $\alpha'_R = 89.0°$ (see Fig. 1 and Table I). The averaged structure is composed of In(1,2), In(3,4), In(5,6), XSe(1), XSe(2,3), X(5,6), and XTe(7,8), where $A(i,j)$ denotes the averaged position of atoms $A(i)$ and $A(j)$ in the pseudocell. Figures 3 and 4 are polyhedral drawings of the averaged structure. In(1,2) is located in 0,0,0 and surrounded by an octahedron of X(5,6) atoms. This octahedron shares edges with six tetrahedra about In(5,6) atoms completed by XSe(2,3) and XTe(7,8). A condition for the formation of this building unit of an octahedron sharing edges with six tetrahedra is the differences in chalcogen sizes. The building units are connected by polyhedra about In(3,4) joined at XSe(1) at $\frac{1}{2}$, $\frac{1}{2}$, $\frac{1}{2}$ (rhombohedral coordinates). These polyhedra are drawn as tetrahedra in Fig. 3 and as trigonal bipyramids in Fig. 4. In the latter description the

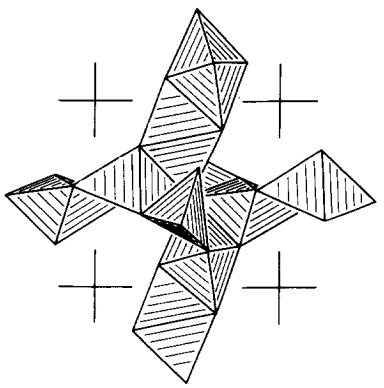

FIG. 4. The chains of trigonal bipyramids of the averaged structure intersecting at XSe(1) (cf. Fig. 3).

equatorial plane is formed by *X*Se(2,3) (two corners) and *X*Te(7,8) with *X*Se(1) and *X*Te(7,8) in the pyramidal apices. In the actual structure the In(4) atoms occupy three of the tetrahedral interstices nearest *X*Se(1), while the In(3) atoms are in the three outer cavities on the opposite side of *X*Se(1). The rhombohedral pseudocell contains three chains of edge-sharing trigonal bipyramids running in the *x*, *y*, and *z* directions, respectively. They intersect at the *X*Se(1) atom, thus connecting the polyhedral units at the apices of the cell, in three dimensions.

In an alternative description all chalcogen atoms are part of either the *X*(5,6) octahedron at the origin or an icosahedron surrounding *X*Se(1). The icosahedra are joined over edge-sharing In(3) tetrahedra (Fig. 2) and the connections between the octahedra and icosahedra are over In(5) and In(6) tetrahedra.

In the present model of the structure In(1) and its environment are disordered as shown in Fig. 5a. The occupancies of the various sites were included in the least-squares refinement and are about $\frac{1}{3}$ for In(1), $\frac{2}{3}$ for *X*Te(5A), $\frac{1}{3}$ for *X*Se(5B), and $\frac{1}{6}$ for *X*Se(4) (cf. Table III). In(1) and *X*Se(4) are located on the threefold axis, near the $\bar{3}$ centers of space group $R\bar{3}$. This means that In(1) is present in two-thirds of the interstices and that *X*Se(4) appears in one-third of them, on either side of the $\bar{3}$ centers. Our interpretation of the disorder is given in Figs. 5b–d: In one-third of the interstices In(1) is in a tetrahedral environment composed of three *X*Te(5A) and one *X*Se(4) atoms as depicted in Fig. 5b. Judging from the interatomic distances, *X*Se(4) have *X*Se(5B) atoms as next nearest neighbors at 3.67(1) Å. Another one-third of the interstices have In(1) in a one-sided coordination of three *X*Te(5A) atoms at 3.076(9) Å with three further *X*Te(5A) at 3.644(9) Å as in Fig. 5c. This polyhedron about In(1) with three short and three long In(1)–*X*Te(5A)

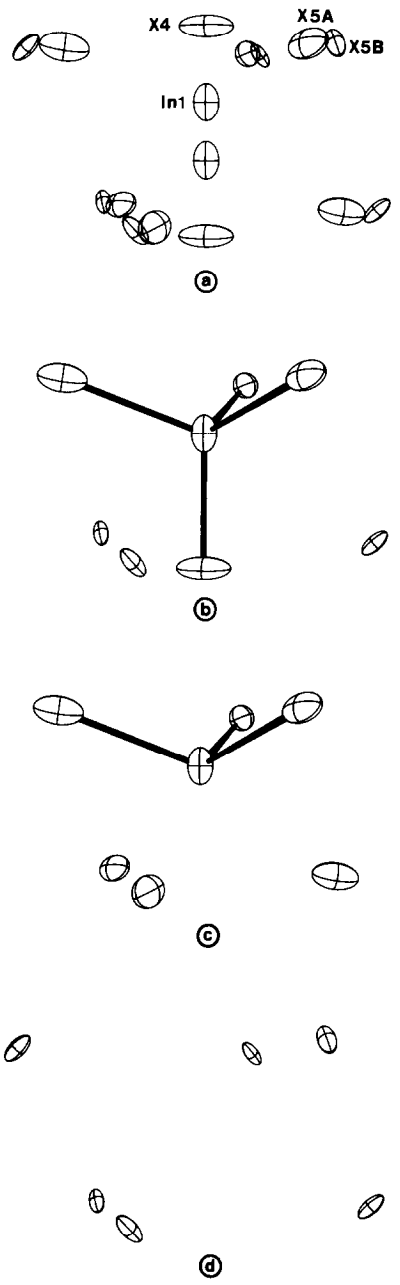

FIG. 5. The In(1) disorder (a) and its interpretation (b–d).

distances is a "type *c* (cation)" octahedron in the description of van der Vorst and Maaskant (*11*); it is indicative of In^{I} with the lone pair of electrons pointing along the

threefold axis toward the uncoordinated XTe(5A) triangle. The In(1) atoms in Fig. 5b are in oxidation state III. Finally, the unoccupied one-third of the interstices are formed by equal amounts of XTe(5A) and XSe(5B) atoms (Fig. 5d). The distances given for In(1) and its neighbors are of course affected by the overlapping electron densities caused by the disorder.

There are three In(1) cavities per unit cell, of which on average one is empty, one includes In^{I}, and one In^{III}. Thus we have a unit cell content of

$$In^{I}In^{III}(oct)_3In^{III}(tetr)_{73}X_{115}$$

or $In_{\sim 2.01}X_3$. For electroneutrality, assuming X^{-II}, one would expect

$$In^{I}_{x}In^{III}(oct)_3In^{III}(tetr)_{75-x}X^{-II}_{117-x}$$

with $0 \leq x \leq 3$ corresponding to the limits In_2X_3 and $In_{2.05}X_3$. Then there are no empty cavities. If we allow for these but neglect the charge compensation, the lower limit is $In_{1.97}X_3$. Electric neutrality would require In^{II} as the In(1) with one-sided coordination, a rather improbable event. We have also found the composition XSe:XTe = 2.22:3 instead of the S:Se:Te $\approx$ 1:2:3 expected from the electron microprobe analysis. This discrepancy has been discussed above.

Discussion

There seems to be no straightforward example of In^{I} coordination in the literature on indium chalcogenides. The structural models are blurred by large thermal vibrations, which we prefer to interpret as actually an average over two or more displaced In positions. Obvious In^{I} environments are found in, e.g., the isostructural In_4Se_3 (*12*) and In_4Te_3 (*13*), where one of the In atoms is in a large cavity formed by seven Se (or Te) atoms and one In atom at distances between 3.0 (3.2) and 3.8 Å. Both the large distances and the large apparent In thermal motion seem to be indicative of In^{I}. Similar In^{I} coordination is shown by InTe (*14*), In_6Se_4 (*15*), and In_6S_7 (*16*). A less obvious situation exists in the present compound with In^{I} in an approximately octahedral interstice. There is apparently only a small difference in volume requirement for In^{III} in octahedral and In^{I} in one-sided trigonal pyramidal coordination with three next nearest neighbors, at least when, as here, Te is the ligand atom. Thus there is a possible exchange of In^{III} for In^{I} complicating the structural models. In order to maintain electroneutrality, vacancies in either cation or anion sites may have to be introduced and so a range of nonstoichiometry is obtained, or alternatively by ordering of the In^{I} atoms or vacancies new phases are formed which can be very close to each other in composition. For example, a phase In_3Te_4 has been proposed (*17*) with ordered cation vacancies and a mixed In^{II}–In^{III} valency, which should, however, rather be In^{I}–In^{III}. Another compound where In^{I} may substitute for In^{III} in octahedral coordination is the γ-In_2S_3 stabilized by As or Sb (*18*). Here the octahedrally coordinated In atoms are off-center along a threefold axis and with three short In–S distances, 2.55 Å, and three long, 2.80 Å. The In thermal vibrations are large along the threefold axis while the S atoms with long In–S distances have thermal ellipsoids which are very much elongated in directions perpendicular to the axis. The general picture is thus very similar to that in the present compound except that the chalcogen is sulfur with resulting shorter bond distances. In conclusion, we believe that some of the ambiguities among the indium chalcogenide compounds are caused by the In^{I}–In^{III} ambivalency.

Acknowledgments

We thank Dr. H. Titze for providing the crystals and the microprobe analysis of their composition. The

Swedish Natural Science Research Council gave financial support.

References

1. H. TITZE, *Acta Chem. Scand. A* **35,** 763 (1981).
2. L. I. MAN, R. M. IMAMOV, AND S. A. SEMILETOV, *Sov. Phys. Crystallogr.* **21,** 355 (1976).
3. S. POPOVIĆ, A. TONEJC, B. GRŽETA-PLENKOVIČ, B. ČELUSTKA, AND R. TROJKO, *J. Appl. Crystallogr.* **12,** 416 (1979).
4. G. A. STEIGMAN, H. H. SUTHERLAND, AND J. GOODYEAR, *Acta Crystallogr.* **19,** 967 (1965).
5. A. LIKFORMAN, D. CARRÉ, AND R. HILLEL, *Acta Crystallogr. Sect. B* **34,** 1 (1978).
6. H. INUZUKA AND S. SUGAIKE, *Proc. Japan Acad.* **30,** 383 (1954).
7. P. MAIN, S. E. HULL, L. LESSINGER, G. GERMAIN, J.-P. DECLERCQ, AND M. M. WOOLFSON, "MULTAN. A Program for the Automatic Solution of Crystal Structures from X-Ray Diffraction Data," Univs. of York, England, and Louvain, Belgium, (1978); M. M. WOOLFSON, *Acta Crystallogr. Sect. A* **33,** 219 (1977).
8. "International Tables for X-Ray Crystallography," Vol IV, Kynoch Press, Birmingham (1974).
9. W. H. ZACHARIASEN, *Acta Crystallogr.* **23,** 558 (1967).
10. R. D. SHANNON, *Acta Crystallogr. Sect. A* **32,** 751 (1976).
11. C. P. J. M. VAN DER VORST AND W. J. A. MAASKANT, *J. Solid State Chem.* **34,** 301 (1980).
12. J. H. C. HOGG, H. H. SUTHERLAND, AND D. J. WILLIAMS, *Acta Crystallogr. Sect. B* **29,** 1590 (1973).
13. J. H. C. HOGG AND H. H. SUTHERLAND, *Acta Crystallogr. Sect. B* **29,** 2483 (1973).
14. J. H. C. HOGG AND H. H. SUTHERLAND, *Acta Crystallogr. Sect. B* **32,** 2689 (1976).
15. J. H. C. HOGG, *Acta Crystallogr. Sect. B* **27,** 1630 (1971).
16. J. H. C. HOGG AND W. J. DUFFIN, *Acta Crystallogr.* **23,** 111 (1967).
17. T. KARAKOSTAS, N. F. FLEVARIS, N. VLACHAVAS, G. L. BLERIS, AND N. A. ECONOMOU, *Acta Crystallogr. Sect. A* **34,** 123 (1978).
18. R. DIEHL, C.-D. CARPENTIER, AND R. NITSCHE, *Acta Crystallogr. Sect. B* **32,** 1257 (1976).